٢٥

GSI

GSI-94-77
PREPRINT
NOVEMBER 1994

SPONTANEOUS-FISSION HALF-LIVES OF DEFORMED SUPERHEAVY NUCLEI

SW 94 51

R. SMOLANCZUK, J. SKALSKI, A. SOBICZEWSKI

CERN LIBRARIES, GENEVA
SCAN-9412197

Gesellschaft für Schwerionenforschung mbH
Postfach 110552 · D-64220 Darmstadt · Germany

Spontaneous-fission half-lives of deformed superheavy nuclei

R. Smolańczuk, J. Skalski and A. Sobiczewski

Soltan Institute for Nuclear Studies, Hoza 69, PL-00-681 Warszawa, Poland

and

Gesellschaft für Schwerionenforschung, D-64220 Darmstadt, Germany

Abstract

Spontaneous-fission half-lives of heaviest nuclei are analyzed in a multidimensional deformation space. They are calculated in a dynamical approach, without any adjustable parameters. The potential energy is obtained by the macroscopic-microscopic method and the inertia tensor by the cranking method. The action integral is minimized by a variational procedure. Even-even nuclei with proton number $Z = 104 - 114$ and neutron number $N = 142 - 176$ are considered.

The results reproduce rather well the existing experimental data for the considered nuclei and predict relatively long half-lives for many nuclei not yet observed, sufficient to detect them if synthesized in a laboratory.

1 Introduction

The objective of the present paper is to analyze the spontaneous-fission properties of deformed superheavy nuclei in a multidimensional deformation space. Such quantities as potential energy (in particular the potential-energy barrier along the fission trajectory), the effective inertia along the fission trajectory and the fission half-life of a nucleus are studied. Even-even nuclei with proton number $Z = 104 - 114$ and neutron number $N = 142 - 176$ are considered.

By deformed superheavy nuclei, we understand here nuclei situated, in the nuclear chart, in the neighbourhood of the nucleus $^{270}108$ (^{270}Hs), which is expected to be a doubly magic deformed nucleus [1, 2]. One of specific properties of these nuclei is that they are expected to be well deformed (e.g. [2]). This puts a requirement to calculate even the ground-state (equilibrium) energy of a nucleus, connected with relatively small

deformations, in a sufficiently large deformation space, in distinction to the case of nuclei which are spherical or nearly spherical in their ground state. Another property is that the fission barriers of these very heavy nuclei are relatively simple and thin. The deformation space required for the analysis of such barriers is importantly smaller than the space required for lighter nuclei, as those with $Z = 92 - 102$, which have much thicker and more complex barriers. In practice, the space used for the analysis of the ground state of the considered nuclei is sufficient also for the analysis of their fission barriers. The third property is that shell effects are extremely important for these nuclei. Most, or may be even all, of them would not exist without these effects [2,3]. This puts a strong requirement of the theory to account for these effects as accurately as possible, both in the potential energy and in the inertia of a nucleus with respect to the fission mode.

Being a region of very heavy nuclei, it still contains a number of nuclei with measured fission half-life, to provide a test for the calculations.

The present analysis belongs to a series of papers [4–6], treating the spontaneous fission in the dynamical way, i.e. taking into account the inertia tensor of a nucleus, when seeking the trajectory along which the probability of the barrier penetration is largest. In the older papers [4,5], another deformation space, more proper for lighter nuclei with $Z = 92 - 102$, has been used, than taken in the present paper. In the more recent analysis [6], the odd-multipolarity deformations β_3 and β_5 have been taken into account, which are not important for the nuclei considered here, while the deformations β_6 and β_8, which are needed for these nuclei, have been omitted. All these differences in the deformation spaces are partly the consequences of the fact that the regions of nuclei considered in the earlier papers [4–6] differ from this discussed here.

An advantage of the dynamical analysis is that it does not use any adjustable parameters. In statical considerations [7–11], a phenomenological inertia function is taken, which has at least one free parameter fitted to experimental data. Additionally, the phenomenological function disregards the shell structure of a nucleus, which is taken into account in the microscopic inertia tensor used in the dynamical approach, and which is so important for the considered nuclei.

The present theoretical paper is closely connected with the intensive experimental activity in recent years on the synthesis and study of the properties of heaviest nuclei (cf. e.g. [12–19]). It aims in the interpretation of existing data and in predictions of properties of nuclei not yet observed.

Some of the results of the present paper have been presented earlier [20–22].

Method of the analysis is described in sect. 2, the results and discussion are given in sect. 3 and conclusions drawn from the study are presented in sect. 4.

2 Method of the calculations

2.1 Potential energy

The potential energy of a nucleus is calculated by the macroscopic-microscopic method. The Yukawa-plus-exponential model [23] with the standard values of its parameters (e.g. [24]) is used for the macroscopic part of the energy. The Strutinski shell correction, based on the Woods-Saxon single-particle potential [25], is taken for the microscopic part. The "universal" variant of the parameters of the potential is chosen (the same as in [2] where they are also specified).

The residual pairing interaction is treated in the usual BCS approximation. The strength of the interaction is taken the same as in [2], where it has been fitted to recent data for nuclear masses.

2.2 Inertia tensor

The inertia tensor describes the inertia of a nucleus with respect to changes of its deformation. We calculate it in the cranking approximation. The corresponding formula is (e.g. [5,26–28])

$$B_{\alpha_i\alpha_j} = 2\hbar^2 \sum_{\nu\nu'} \frac{< \nu|\partial H/\partial\alpha_i|\nu' >< \nu'|\partial H/\partial\alpha_j|\nu >}{(E_\nu + E_{\nu'})^3}(u_\nu v_{\nu'} + u_{\nu'} v_\nu)^2 + P^{ij} \ , \qquad (1)$$

where α_i and α_j are the deformation parameters, H is the single-particle hamiltonian, u_ν and v_ν are the BCS variational parameters and E_ν is the quasi-particle energy corresponding to the single-particle state $|\nu >$. The term P^{ij} describes the effect of the collective motion on the pairing interaction. Various properties of the tensor $B_{\alpha_i\alpha_j}$ have been discussed in [5,26–29].

The inertia tensor provides metric in the deformation space, when calculating the penetration of a nucleus through the fission barrier.

2.3 Spontaneous-fission half-life

The spontaneous-fission half-life $T_{\rm sf}$ is calculated by the formula

$$T_{\rm sf} = T_0 \, P^{-1} \ , \qquad (2)$$

where P is the probability of the barrier penetration by a nucleus and T_0 is the half-life when this probability is equal to unity. The half-life T_0 is determined by the number of assaults of a nucleus on the fission barrier in unit time, $\omega_0/2\pi$,

$$T_0 = 2\pi ln2/\omega_0 \ , \qquad (3)$$

and, thus, by the zero-point vibration energy of it in the fission degree of freedom, $E_{\rm zp} = 0.5\,\hbar\omega_0$.

The probability P is obtained in the semiclassical (WKB) approximation

$$P = [1 + \exp 2S(L)]^{-1} \,, \tag{4}$$

where the action integral $S(L)$ along a one-dimensional trajectory L in a multidimensional deformation space is

$$S(L) = \int_{s_1}^{s_2} \{\frac{2}{\hbar^2} B_L(s)[E_L(s) - E_0]\}^{\frac{1}{2}} ds \,. \tag{5}$$

Here, $E_L(s)$ is the potential energy, $B_L(s)$ is the effective inertia, both along the trajectory L, and E_0 is the energy of a fissioning nucleus. The parameter s specifies the position of a point on the trajectory L, with s_1 and s_2 corresponding to the entrance and exit points of the barrier, i.e. to the classical turning points determined by: $E_L(s) = E_0$. The effective inertia $B_L(s)$ associated with the fission motion along the trajectory L is

$$B \equiv B_L(s) = \sum_{ij} B_{\alpha_i\alpha_j}(s) \frac{d\alpha_i}{ds} \frac{d\alpha_j}{ds} \,, \tag{6}$$

where $B_{\alpha_i\alpha_j}$ are components of the inertia tensor, eq. (1), and α_i, α_j are the deformation parameters (β_λ).

The half-life $T_{\rm sf}$ is calculated in the dynamical way (e.g. [5,30]), i.e. along the dynamical trajectory $L_{\rm dyn}$, for which the action integral $S(L)$ is minimal, with full dependence of the inertia tensor $B_{\alpha_i\alpha_j}$ on the deformation taken into account.

2.4 Deformation space

Axially symmetric shapes are used in our analysis of spontaneous fission. These shapes are described by the usual deformation parameters β_λ, appearing in the expression for nuclear radius (in the intrinsic frame of reference) in terms of spherical harmonics $Y_{\lambda 0}(\vartheta)$,

$$R(\vartheta) = R_0(\beta_\mu)[1 + \sum_\lambda \beta_\lambda Y_{\lambda 0}(\vartheta)] \,, \tag{7}$$

where the dependence of R_0 on β_μ is determined by the volume-conservation condition.

The reason to disregard the axially asymmetric shapes lies in the dynamical treatment of fission. Along the static trajectory (i.e. the trajectory along which the potential enegy is minimal), the potential energy is usually decreased by the non-axial (γ) deformation by up to about 1 MeV [4,31,32]. The effective inertia B, eq. (6), is, however, large along this trajectory and leads to a larger action integral than that along the trajectory with $\gamma = 0$. This has been directly shown in [32] for the nucleus $^{260}106$ (^{260}Sg), from the region considered here, and in [4] for a lighter nucleus.

Concerning the axial deformations β_λ, we find, similar to [33], that it is sufficient to consider the deformations of the multipolarities up to $\lambda = 8$. The contribution of β_9 and β_{10} to the potential energy is already negligible. The deformations with odd multipolarities $\lambda = 3, 5, 7$ contribute to the energy already behind the thin fission barriers of these very heavy nuclei, considered here. Thus, the potential energy is analyzed finally in the 4-dimensional deformation space $\{\beta_\lambda\}$, $\lambda = 2, 4, 6, 8$.

2.5 Details of the calculations

The potential energy E and the inertia tensor $B_{\beta_\lambda\beta_\mu}$, eq. (1), are calculated individually for each nucleus. No averaging over proton Z and neutron N numbers is used.

The potential energy E is calculated at grid points (β_2, β_4) with steps: $\Delta\beta_2 = \Delta\beta_4 = 0.05$. The range of both β_2 and β_4 is taken individually for each nucleus, to obtain the whole region of the fission barrier.

The dynamical calculations of $T_{\rm sf}$ are performed in the approximation tested in [32]. These are the calculations performed in 2-dimensional deformation space $\{\beta_\lambda\}$, $\lambda = 2, 4$, but with the potential energy E minimized at each point (β_2, β_4) of this space in the remaining degrees of freedom: β_6 and β_8. Thus, the potential energy, and correspondingly the inertia tensor, are

$$E(\beta_2, \beta_4; \beta_\nu^m) \,, \qquad\qquad B_{\beta_\lambda\beta_\mu}(\beta_2, \beta_4; \beta_\nu^m) \,, \tag{8}$$

where β_ν^m, $\nu = 6, 8$, is the value of β_ν, at which the energy E is minimal at the point (β_2, β_4). A detailed study [32] of dynamics in deformation spaces of various dimensions has shown that this approximation is quite good for nuclei considered in the present paper.

To get sufficiently accurate fission trajectory, the values of the potential energy E and of the inertia tensor $B_{\beta_\lambda\beta_\mu}$ of eq. (8) are interpolated (by the standard procedure SPLIN3 of the IMSL library) to the more dense grid: $\Delta\beta_2 = 0.01, \Delta\beta_4 = 0.0025$. Only on such dense grid, the variational calculation has been performed, using a dynamical-programming method described in [5].

To calculate the ground-state energy E_0 of a nucleus (eq. (5))

$$E_0 = E(\beta_\lambda^0) + E_{\rm zp}, \tag{9}$$

the zero-point energy in the fission degree of freedom is taken as: $E_{\rm zp} = 0.7$ MeV. This is the value close to that calculated in [2]. Here, $E(\beta_\lambda^0)$ is the value of the potential energy at the equilibrium (ground-state) deformation β_λ^0. The energy $E_{\rm zp}$ determines simultaneously the number of assaults of a nucleus on the fission barrier, according to eq. (3).

3 Results and discussion

3.1 Potential energy and fission trajectory

Fig. 1 illustrates a map of the potential energy by the example of the recently synthesized [17,18] nucleus $^{266}106$ (^{266}Sg), which is closest, among observed even-even nuclei, to the predicted [1,2] doubly magic deformed nucleus $^{270}108$ (^{270}Hs). This is also the isotope of the element 106 (Sg) by which the chemical properties of this element are planned to be studied [34]. At each point (β_2, β_4), the energy is minimized in β_6 and β_8 degrees of freedom.

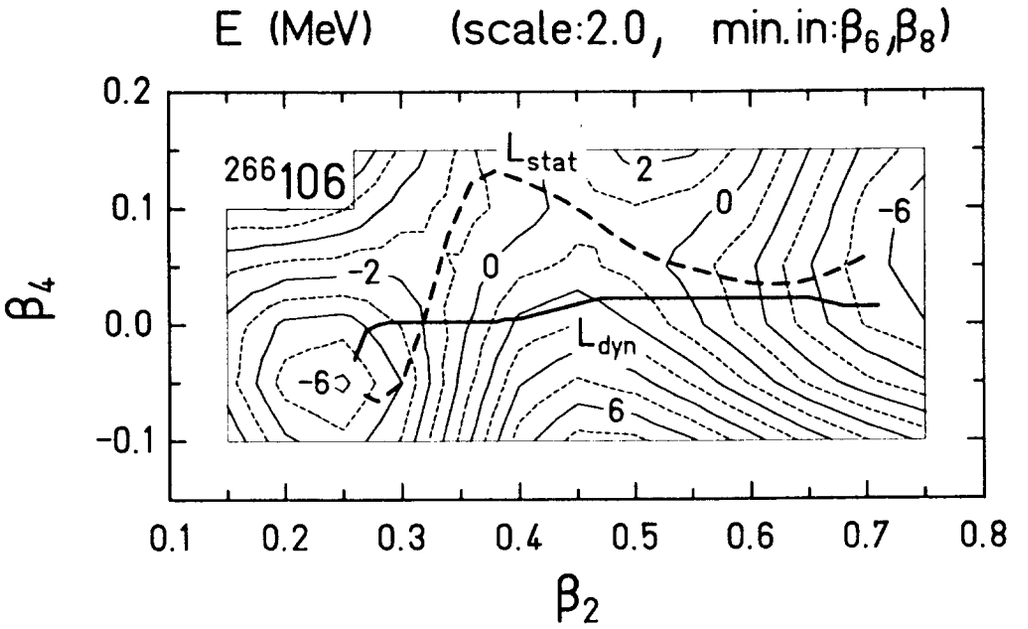

Figure 1: Contour map of the potential energy E calculated as a function of the deformations β_2 and β_4, for the nucleus $^{266}106$ (^{266}Sg). At each point (β_2, β_4), the energy is minimized in β_6 and β_8 degrees of freedom. Numbers at the contour lines give the values of the energy. Difference in the values between neighbouring solid lines (scale) is 2 MeV. Dashed lines divide this difference by two. Dynamical, $L_{\rm dyn}$, and statical, $L_{\rm stat}$, fission trajectories are shown.

The dynamical fission trajectory $L_{\rm dyn}$ is also shown in the Fig. 1. It has a tendency to be close to a straight line and to have a possible small slope with respect to the β_2-axis, as both these features lead to a small effective inertia B, eq. (6), along the trajectory and, consequently, to a small action integral. The small slope corresponds to a small contribution to B of the components $B_{\beta_\lambda \beta_\mu}$ of the inertia tensor with $\lambda, \mu > 2$, according to eq. (6). A large curvature or a large slope of the dynamical trajectory may appear only at the beginning or at the end of the barrier, where the potential energy is small and

a large value of B is not so important.

The static trajectory $L_{\rm stat}$ is also shown in Fig. 1, for comparison. The effective inertia B is usually large along this trajectory, as discussed in [32], and, in spite of smaller fission barrier, leads to a larger action than that along the dynamical trajectory.

3.2 Fission barrier

Shape of the fission barrier calculated along the dynamical trajectory $L_{\rm dyn}$ is illustrated in Fig. 2. One can see that the barrier is thin. It ends at a deformation $\beta_2 \approx 0.7$, thus at about the deformations of fission isomers, i.e. the deformations at which the second minimum in energy appears for lighter nuclei, around americium. The barrier is, however, high. This is mainly due to a large (in absolute value), negative shell correction $E_{\rm sh}$ to the ground-state energy. For the considered nucleus $^{266}106$, the correction is: $E_{\rm sh} = -6.3$ MeV.

The (static) barrier, calculated along the static trajectory $L_{\rm stat}$, is also shown in Fig. 2, for comparison. This barrier is important for calculations of the competition between neutron emission and fission (Γ_n/Γ_f) of an excited nucleus.

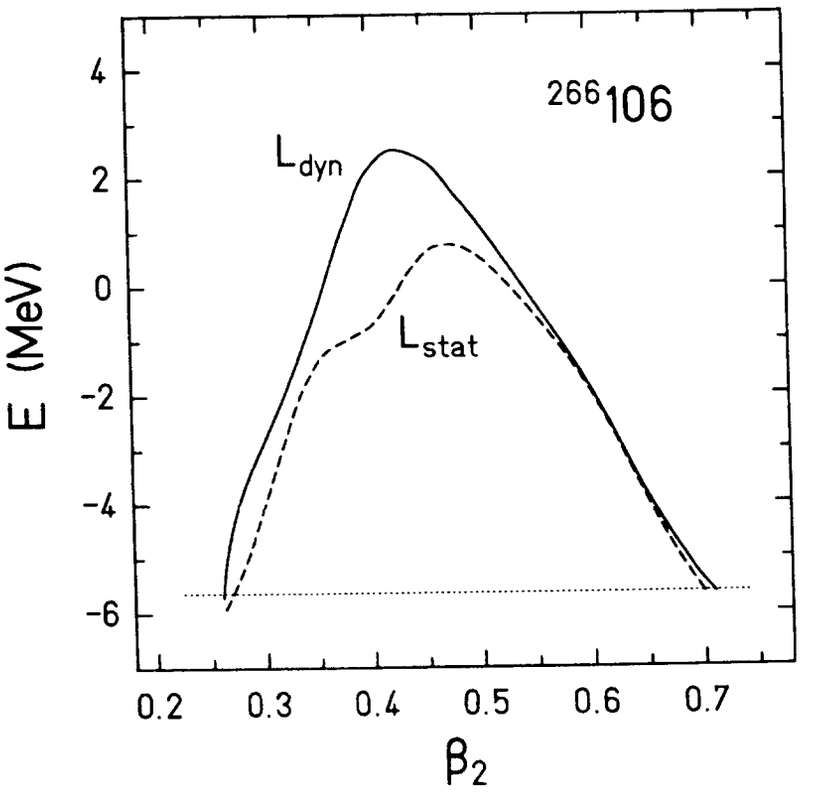

Figure 2: Shape of the potential-energy barrier calculated along the dynamical and statical fission trajectories, for the nucleus $^{266}106$.

One can see in Fig. 2 that the static barrier is by almost 2 MeV lower, and it also much differs in shape from the dynamical barrier. The height of the statical barrier is about equal to the ground-state shell correction $E_{\rm sh}$, as there is almost no contribution of the smooth part of the energy to this height, and the shell correction at the saddle point is rather small, as discussed in [3].

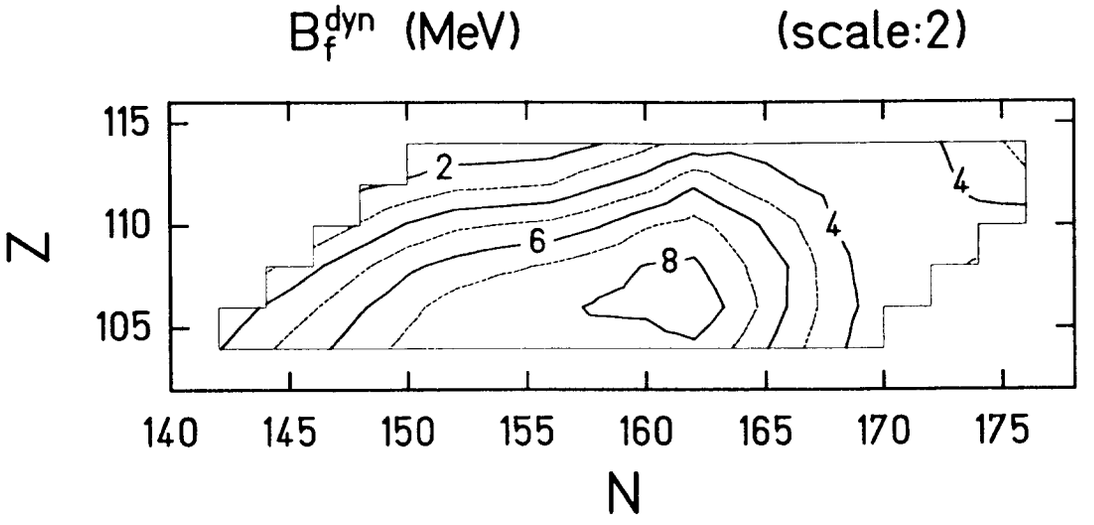

Figure 3: Contour map of the height of the dynamical fission barrier, $B_f^{\rm dyn}$, plotted as a function of the proton Z and neutron N numbers.

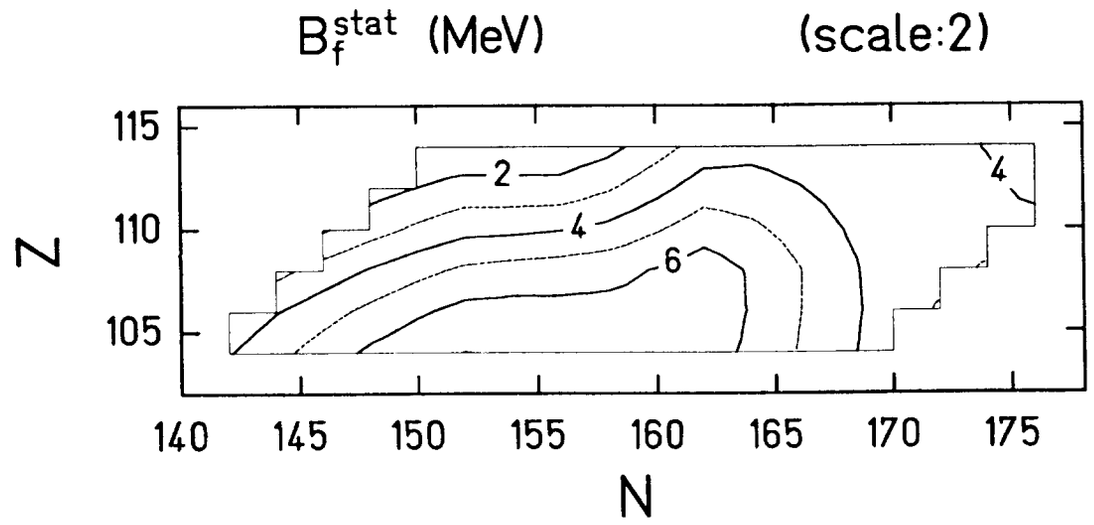

Figure 4: Same as in Fig. 3, but for the static fission barrier $B_f^{\rm stat}$.

Contour map of the height $B_f^{\rm dyn}$ of the dynamical fission barrier is shown in Fig. 3. As mentioned above, the height is large. It is larger than 7 MeV for about 20 of the

nuclei considered. The largest value, 8.8 MeV, is obtained for the nucleus $^{268}106$, i.e. the nucleus with the neutron number $N = 162$, corresponding to the predicted closed deformed neutron shell.

Contour map of the height $B_f^{\rm stat}$ of the static fission barrier is given in Fig. 4. One can see that Fig. 4 presents a "mountain", which is flattened to some degree with respect to the "mountain" of $B_f^{\rm dyn}$ (Fig. 3). It is decreased around the top (by up to about 2 MeV), while it remains almost unchanged at the bottom, in comparison with $B_f^{\rm dyn}$.

As the main contribution to the barrier heights $B_f^{\rm dyn}$ and $B_f^{\rm stat}$ is the ground-state shell correction $E_{\rm sh}$, it is interesting to see also the map of the latter quantity. This is shown in Fig. 5. One can see a really strong correlation between the three maps.

It is worth noting in Fig. 5 that, when moving from lighter to heavier nuclei, after the maximum (in absolute value) of $E_{\rm sh}$, obtained for the predicted doubly magic deformed nucleus $^{270}108$, one observes a minimum of this quantity for $N \approx 170$ and then one sees its increase again, when approaching the predicted doubly magic spherical nucleus $^{298}114$. The corresponding behaviour is also observed in the fission-barrier heights in Fig. 3 and Fig. 4.

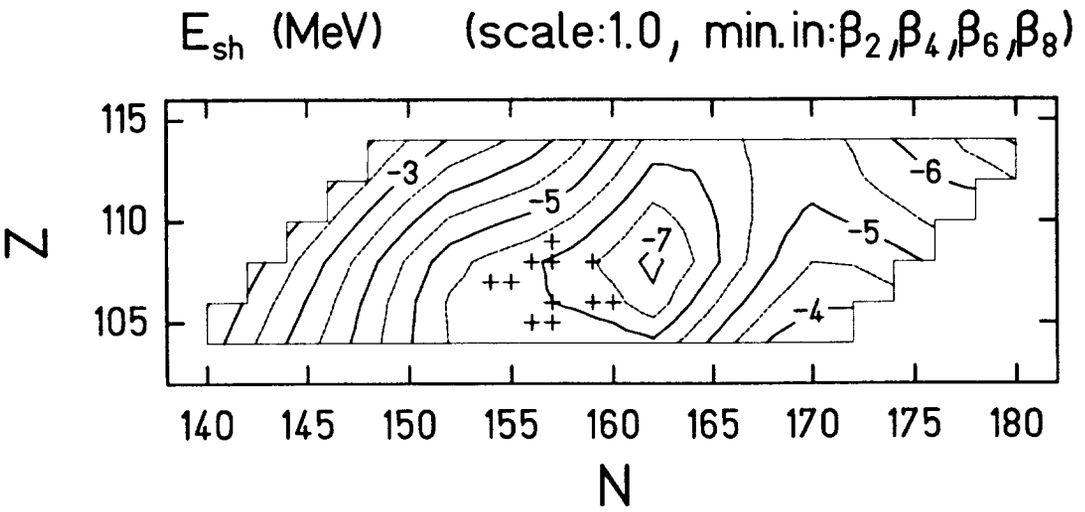

Figure 5: Contour map of the ground-state shell correction, $E_{\rm sh}$, to the potential energy E. Crosses indicate the heaviest nuclei synthesized up to now.

3.3 Effective inertia

The effective inertia B, eq. (6), calculated along the dynamical fission trajectory $L_{\rm dyn}$ is shown in Fig. 6. One can see that it is a rather strongly fluctuating function of deformation. This is because the inertia tensor (mass parameters) is a much less collective quantity than the potential energy or even the moment of inertia (i.e. the inertia of a

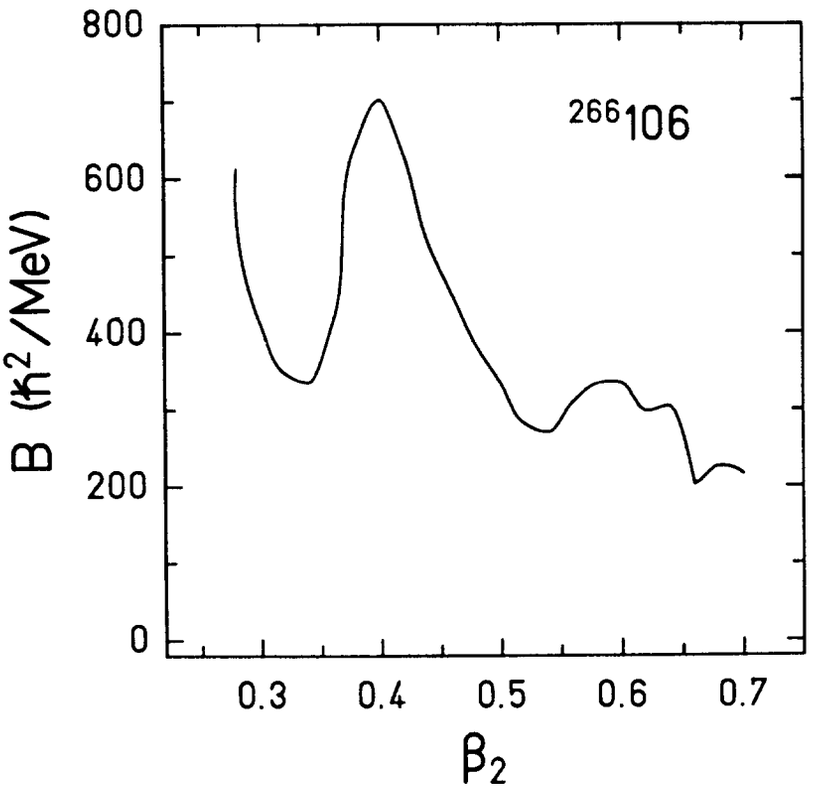

Figure 6: Effective inertia B calculated along the dynamical fission trajectory, for the nucleus $^{266}106$.

nucleus with respect to its rotation) as was discussed in detail in [28]. Thus, it is very sensitive to the internal, single-particle structure of a nucleus which changes with its deformation. A general tendency is that the inertia tensor is small at deformations at which the potential energy has deep minima (low single-particle-level density at the Fermi level at these deformations) and large at deformations at which the potential energy has particularly large values, e.g. maxima or saddle points (high single-particle-level density at these points). This means that the regions around the maxima in the potential energy along the fission trajectory, giving the largest contribution to the half-life $T_{\rm sf}$ due to large both the potential energy E and the inertia B, should be especially carefully treated in the calculations of this half-life.

3.4 Fission half-life

Contour map of logarithm of the fission half-life $T_{\rm sf}$, given in seconds, is shown in Fig. 7. The structure of the map is similar to that of the barrier height $B_f^{\rm dyn}$ (Fig. 3).

One can see that the half-lives are rather large. The largest value, obtained for $^{268}106$, is of the order of few hours (3.5 h). (Even larger values are obtained only for transitional

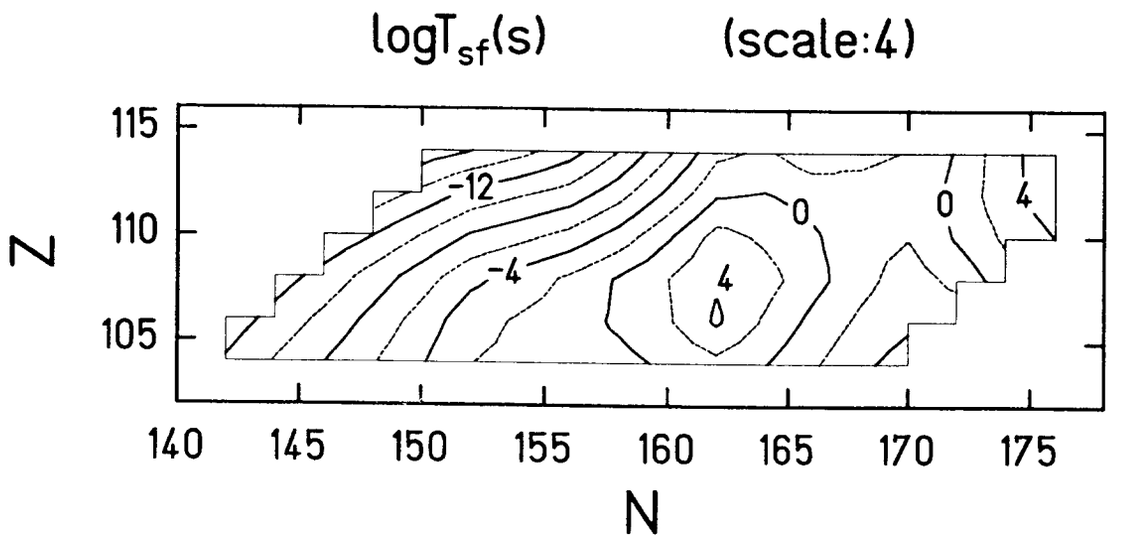

Figure 7: Same as in fig. 3, but for logarithm of the spontaneous-fission half-life T_{sf}, given in seconds.

nuclei, $N > 174$, on the border with the region of spherical superheavy nuclei situated around the nucleus $^{298}114$.)

Fig. 8 shows the dependence of logarithm of the fission half-life T_{sf} on the neutron number N, for all considered values of Z. The α-decay half-life T_α is also shown, for completeness. The latter is calculated in the same way as in [2], with small improvements. One can see a clear effect of the $N = 162$ shell in the fission half-life T_{sf}, for all Z. The effect is especially strong for $Z = 106$. For $Z = 104$, also the effect of the lower shell at $N = 152$ is visible. The effect of $N = 162$, and smaller effect of $N = 152$, are also seen in the α-decay half-life T_α.

The existing experimental values of both T_{sf} and T_α are rather well reproduced by the calculations. This may be considered as a satisfying result as there are no free parameters in the calculations, fitted to experiment.

A comparison between the calculated T_{sf} and T_α shows that for $Z = 104$ T_{sf} is smaller than T_α for all N. For $Z = 106$, T_{sf} is comparable with T_α for a large number of isotopes ($N = 154 - 164$). For higher Z, it is even larger than T_α and for even larger number of isotopes. This seems to be the effect of shells, mainly of that at $N = 162$, to which T_{sf} is more sensitive than T_α. Only for lightest isotopes, T_{sf} is shorter than T_α for all investigated elements.

The results are generally similar to the earlier ones [8], obtained in a smaller deformation space. The present values of T_{sf} are significantly lower, however, for $Z = 108$ and 110 than the previous ones. This is probably mainly due to lower values of the dynamical effective inertia, presently used, than those of the phenomenological inertia, exploited previously [8].

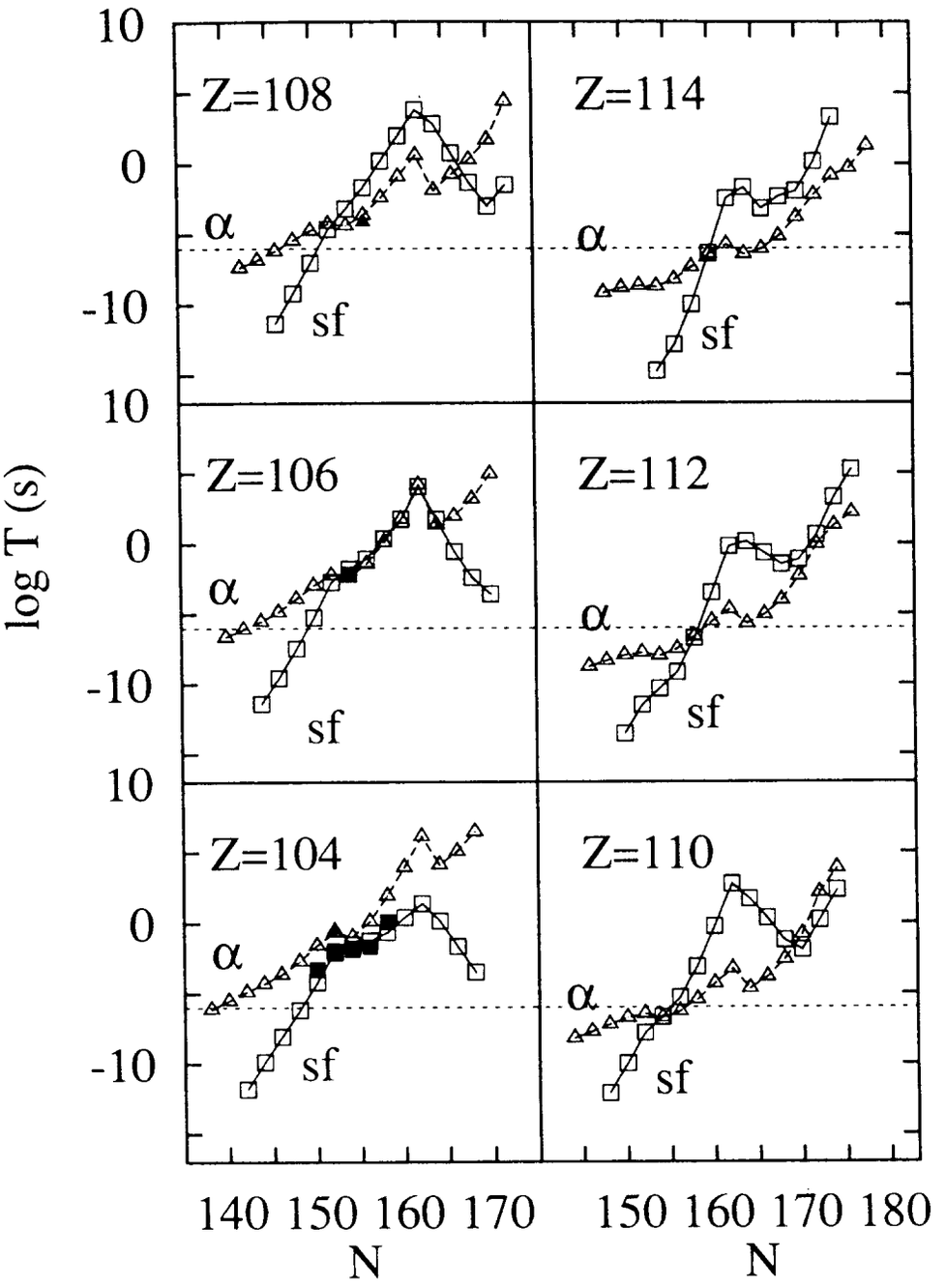

Figure 8: Dependence of logarithm of the calculated spontaneous-fission (sf) half-lives, given in seconds, on the neutron number N, for elements 104–114. The α-decay half-lives (α) are also shown, for comparison. Experimental values are given by full points. The horizontal dashed line indicates about the lowest half-life (1 μs) of a nucleus, which can be detected in a present-day set-up, after its synthesis.

More detailed calculated fission properties of the considered nuclei are given in Table 1. The first three columns of the Table 1 specify the proton Z, neutron N and mass A numbers of a nucleus, respectively. The fourth one gives the equilibrium value of the

Table 1. Equilibrium deformation and spontaneous-fission properties of nuclei specified in the first three columns.

Z	N	A	β_2^0	β_2^{en}	β_2^{ex}	B_f^{stat} (MeV)	B_f^{dyn} (MeV)	$\log T_{sf}(s)$	T_{sf}	T_{sf}^{exp}	Ref.
104	142	246	.238	.30	.56	3.9	4.0	-11.81	1.5 ps		
104	144	248	.239	.29	.57	4.7	4.9	-9.87	0.13 ns		
104	146	250	.242	.28	.58	5.5	5.7	-8.07	8.5 ns		
104	148	252	.245	.28	.60	6.2	6.6	-6.19	.65 μs		
104	150	254	.248	.28	.63	6.7	7.3	-4.22	60 μs	$0.5^{+0.2}_{-0.2}$ ms	[35]
104	152	256	.249	.28	.66	7.0	7.9	-2.04	9.1 ms	$7.4^{+0.9}_{-0.7}$ ms	[36]
104	154	258	.248	.27	.68	6.9	7.9	-1.56	28 ms	13^{+3}_{-3} ms	[37]
104	156	260	.247	.27	.68	6.6	7.8	-1.27	54 ms	21^{+1}_{-1} ms	[37]
104	158	262	.243	.27	.69	6.5	7.6	-0.67	0.21 s	$1.2^{+1.0}_{-0.5}$ s	[17,18]
104	160	264	.237	.26	.69	6.4	7.6	0.39	2.5 s		
104	162	266	.229	.26	.70	6.5	7.8	1.37	23 s		
104	164	268	.221	.25	.69	5.7	6.8	0.14	1.4 s		
104	166	270	.203	.24	.67	4.9	5.4	-1.69	20 ms		
104	168	272	.196	.23	.66	4.2	4.2	-3.50	0.32 ms		
106	144	250	.239	.29	.55	3.9	4.1	-11.40	4.0 ps		
106	146	252	.242	.28	.56	4.6	4.9	-9.56	0.28 ns		
106	148	254	.244	.28	.58	5.3	5.9	-7.45	35 ns		
106	150	256	.247	.27	.62	5.9	6.7	-5.24	5.8 μs		
106	152	258	.248	.27	.66	6.3	7.5	-2.74	1.8 ms		
106	154	260	.247	.27	.68	6.4	7.8	-1.79	16 ms	$7.2^{+4.8}_{-2.7}$ ms	[38]
106	156	262	.244	.27	.69	6.3	7.8	-1.07	85 ms		
106	158	264	.244	.26	.70	6.3	8.1	0.37	2.3 s		
106	160	266	.239	.26	.71	6.4	8.2	1.76	58 s		
106	162	268	.234	.25	.73	6.8	8.8	4.10	3.5 h		
106	164	270	.225	.25	.70	5.9	7.5	1.74	55 s		
106	166	272	.213	.25	.68	5.0	5.9	-0.54	0.29 s		
106	168	274	.198	.24	.67	4.2	4.4	-2.41	3.9 ms		
106	170	276	.171	.22	.66	3.6	3.6	-3.58	0.26 ms		
108	146	254	.240	.28	.54	3.4	3.8	-11.35	4.5 ps		
108	148	256	.241	.28	.56	4.1	4.8	-9.20	0.63 ns		
108	150	258	.243	.27	.59	4.7	5.8	-7.02	95 ns		
108	152	260	.244	.27	.63	5.2	6.4	-4.63	23 μs		
108	154	262	.243	.27	.66	5.4	6.8	-3.18	0.66 ms		
108	156	264	.242	.26	.68	5.5	7.1	-1.67	21 ms		
108	158	266	.241	.26	.70	5.7	7.7	0.21	1.6 s		
108	160	268	.237	.26	.72	6.1	8.0	1.98	1.6 m		
108	162	270	.233	.25	.73	6.5	8.2	3.82	1.8 h		
108	164	272	.227	.25	.71	5.9	7.1	2.82	11 m		
108	166	274	.217	.24	.69	5.1	6.0	0.76	5.8 s		
108	168	276	.200	.23	.68	4.2	4.2	-1.34	46 ms		
108	170	278	.175	.22	.67	3.5	3.5	-3.01	0.98 ms		
108	172	280	.135	.19	.67	3.3	3.3	-1.49	32 ms		

Table 1 (Continued).

Z	N	A	β_2^0	β_2^{en}	β_2^{ex}	B_f^{stat} (MeV)	B_f^{dyn} (MeV)	$\log T_{sf}(s)$	T_{sf}	T_{sf}^{exp}	Ref.
–	–	–	–	–	–						
110	148	258	.236	.28	.53	2.6	3.1	-12.11	0.78 ps		
110	150	260	.237	.28	.56	3.2	4.1	-9.99	0.10 ns		
110	152	262	.241	.27	.59	3.7	4.8	-7.83	15 ns		
110	154	264	.238	.27	.62	3.8	5.1	-6.69	0.20 μs		
110	156	266	.234	.27	.64	3.9	5.3	-5.32	4.8 μs		
110	158	268	.229	.26	.66	4.3	5.9	-3.14	0.72 ms		
110	160	270	.227	.25	.68	4.9	6.9	-0.27	0.54 s		
110	162	272	.226	.24	.70	5.6	7.4	2.75	9.4 m		
110	164	274	.217	.24	.69	5.2	6.4	1.68	48 s		
110	166	276	.207	.23	.68	4.6	5.2	0.32	2.1 s		
110	168	278	.198	.22	.67	4.0	4.0	-1.25	56 ms		
110	170	280	.153	.21	.66	3.5	3.5	-1.92	12 ms		
110	172	282	.125	.18	.66	3.4	3.5	0.19	1.5 s		
110	174	284	.116	.15	.67	3.5	3.6	2.32	3.5 m		
112	150	262	.232	.29	.53	2.0	2.2	-13.55	28 fs		
112	152	264	.234	.28	.56	2.4	2.7	-11.49	3.2 ps		
112	154	266	.227	.27	.58	2.3	2.8	-10.32	48 ps		
112	156	268	.223	.27	.60	2.3	3.0	-9.16	0.69 ns		
112	158	270	.219	.26	.63	2.9	3.8	-6.73	0.19 μs		
112	160	272	.219	.25	.65	3.7	4.5	-3.50	0.32 ms		
112	162	274	.221	.24	.68	4.5	5.9	-0.20	0.63 s		
112	164	276	.206	.23	.67	4.4	4.8	0.13	1.3 s		
112	166	278	.202	.22	.66	4.1	4.1	-0.67	0.21 s		
112	168	280	.191	.21	.65	3.6	3.7	-1.47	34 ms		
112	170	282	.144	.19	.65	3.4	3.5	-1.15	71 ms		
112	172	284	.123	.17	.66	3.4	3.5	0.60	4.0 s		
112	174	286	.095	.15	.66	3.7	4.3	3.29	32 m		
114	154	268	.219	.28	.54	1.2	1.3	-14.71	1.9 fs		
114	156	270	.209	.26	.56	1.3	1.4	-12.84	0.14 ps		
114	158	272	.207	.25	.60	1.7	1.9	-9.98	0.10 ns		
114	160	274	.208	.24	.62	2.5	2.7	-6.34	0.46 μs		
114	162	276	.212	.23	.64	3.4	3.4	-2.46	3.5 ms		
114	164	278	.203	.22	.65	3.6	3.7	-1.66	22 ms		
114	166	280	.190	.23	.65	3.5	3.6	-3.17	0.68 ms		
114	168	282	.182	.21	.64	3.2	3.4	-2.33	4.7 ms		
114	170	284	.143	.19	.64	3.1	3.3	-1.93	12 ms		
114	172	286	.121	.17	.65	3.3	3.8	0.17	1.5 s		
114	174	288	.086	.14	.66	4.1	4.7	3.32	35 m		

quadrupole component of the deformation β_2^0. This main component of the deformation of a nucleus is chosen to parametrize the position of a point on the fission trajectory. Columns 5 and 6 give the entrance and exit points to and from the barrier, respectively, and columns 7 and 8 give the heights of the static and dynamic barriers. Logarithm of the fission half-life (given in seconds), $\log_{10}T_{\rm sf}(s)$, is presented in column 9 and the half-life itself in column 10. Columns 11 and 12 give experimental values of $T_{\rm sf}$ and the respective references.

One can see in Table 1 that the theoretical values reproduce the experimental results rather well, within a factor of 3, on the average. The largest discrepancy is obtained for the nucleus $^{254}104$, for which the theoretical value is smaller than the experimental one by a factor of 8. Preliminary results of more recent measurements [39] give, however, value [40] which is closer to the calculated value.

A comparison of our half-lives with other calculated values, those of [9], shows that those values are smaller than ours by up to about 8 orders of magnitude. Also the results of [10,41] are very different from ours. For nuclei with neutron number N close to the magic value $N = 162$, the half-lives $T_{\rm sf}$ of [10,41] are smaller than ours by up to more than 6 orders of magnitude. The difference seems to come mainly from smaller phenomenologic inertia taken in [9,10,41] than the microscopic inertia obtained in the present paper.

One can see in Table 1 that almost all considered nuclei are well deformed (large β_2^0). Only the heaviest isotopes, especially those of the elements with largest Z, are transitional. The barriers are thin, especially those of the most neutron-deficient isotopes. Some of these barriers end at quite small deformations $\beta_2 \approx 0.55 - 0.60$. The static fission barrier is systematically lower than the dynamical one by up to about 2 MeV.

3.5 A remark on terminology

It seems to be practical to have some name for the very specific region of nuclei considered in the present paper, due to its specifics and also to a large recent activity, both experimental and theoretical, in the study of these nuclei. The name "deformed superheavy nuclei" is one, a rather natural, of the possibilities. It has been already used for some time [42]. It makes use of the suggestion of P. Armbruster [43,44] to extend the name "superheavy nuclei", primarily reserved [45] for spherical nuclei around the hypothetical doubly magic nucleus $^{298}114$, to all nuclei with very large Z and N, which exist or are expected to exist only due to their shell effects. It looks from recent calculations that the discussed nuclei fulfil this condition. The adjective "deformed" reflects their expected shape and distinguishes them from the "traditional" superheavy nuclei around $^{298}114$, which should be called "spherical superheavy nuclei". Such distinction could not be made by names of elements, as some isotopes of a given element (e.g. 108 (Hs) or 109 (Mt)) belong to one (e.g. deformed) and others to the second (spherical) region of nuclei.

There has been also used the name "rock" [41], at least for a part of the discussed region of nuclei, proposed in connection with their increased stability.

4 Conclusions

The following conclusions may be drawn from the present study:

(1) Almost all considered nuclei are predicted to be deformed. Only very few of them, the heaviest ones, are expected to be transitional.

(2) The ground-state fission barriers of the nuclei are thin. They already end at deformations $\beta_2 \approx 0.55 - 0.70$.

(3) The barriers are, however, high. For about 20 of the considered nuclei, the dynamical fission barrier is higher than 7 MeV. The largest value, 8.8 MeV, is obtained for the nucleus $^{268}106$ (^{268}Sg), i.e. the nucleus with the predicted closed neutron shell at $N = 162$. The static barriers are by up to about 2 MeV lower than the dynamical ones.

(4) The large height of the fission barrier is mainly due to a large shell correction to the ground-state energy of these nuclei. The largest (negative) value of this correction, -7.2 MeV, is obtained for the nucleus $^{270}108$ (^{270}Hs), predicted to be a doubly magic deformed nucleus.

(5) Due to high barriers, the spontaneous-fission half-lives T_{sf} of the considered nuclei are rather large. The largest value, 3.5 h, is obtained for the nucleus $^{268}106$.

(6) The existing experimental values of T_{sf}, for nuclei in the considered region, are rather well reproduced by the calculations.

(7) A comparison between the calculated fission, T_{sf}, and α-decay, T_α, half-lives shows that for $Z = 104$ T_{sf} is smaller than T_α, $T_{sf} < T_\alpha$, for all N. For $Z = 106$, $T_{sf} \approx T_\alpha$ for a large number of isotopes ($N = 154 - 164$). For higher Z, T_{sf} is even larger than T_α and for even larger number of isotopes. Only for the most neutron-deficient isotopes of considered elements, T_{sf} is smaller than T_α.

(8) Thus, the results show that many of not yet observed nuclei in the considered region are expected to have sufficiently long half-lives to be observed in a present-day experimental set-up, if synthesized.

The authors would like to thank Peter Armbruster, Sigurd Hofmann, Gottfried Münzenberg, Wolfgang Nörenberg and Matthias Schädel for many valuable discussions and suggestions. They are also grateful to D.C. Hoffman, E.K. Hulet, Yu.A. Lazarev, R.W. Lougheed, V. Ninov, Yu.Ts. Oganessian, Z. Patyk, A.G. Popeko, W. Reisdorf, P. Rozmej, S. Saro and A.V. Yeremin for helpful discussions. A support by the Polish Committee for Scientific Research (KBN), grant no. 209 549 101, and by GSI-Darmstadt is gratefully acknowledged.

References

[1] Z. Patyk and A. Sobiczewski, Phys. Lett. **B256**, 307 (1991).

[2] Z. Patyk and A. Sobiczewski, Nucl. Phys. **A533**, 132 (1991).

[3] Z. Patyk, A. Sobiczewski, P. Armbruster, and K.-H. Schmidt, Nucl. Phys. **A491**, 267 (1989).

[4] A. Baran, K. Pomorski, S.E. Larsson, P. Möller, S.G. Nilsson, J. Randrup, and A. Sobiczewski, in *Proceedings of the 3rd International Conference on Nuclei Far From Stability*, Cargèse, 1976, (CERN 76-13, Geneva, 1976), p. 537.

[5] A. Baran, K. Pomorski, A. Lukasiak, and A. Sobiczewski, Nucl. Phys. **A361**, 83 (1981).

[6] Z. Patyk, J. Skalski, A. Sobiczewski, and S. Ćwiok, Nucl. Phys. **A502**, 591c (1989).

[7] J. Randrup, S.E. Larsson, P.Möller, S.G. Nilsson, K. Pomorski, and A. Sobiczewski, Phys. Rev. **C13**, 229 (1976).

[8] K. Böning, Z. Patyk, A. Sobiczewski, and S. Ćwiok, Z. Phys. **A325**, 479 (1986).

[9] P. Möller, J.R. Nix, and W.J. Swiatecki, Nucl. Phys. **A469**, 1 (1987).

[10] P. Möller, J.R. Nix, and W.J. Swiatecki, Nucl. Phys. **A492**, 349 (1989).

[11] S. Ćwiok and A. Sobiczewski, Z. Phys. **A342**, 203 (1992).

[12] G. Münzenberg, Rep. Prog. Phys. **51**, 57 (1988).

[13] D.C. Hoffman and L.P. Somerville, in *Particle emission from nuclei*, eds. D.N. Poenaru and M.S. Ivascu, vol.3 (CRC Press, Boca Raton, 1989), p. 1.

[14] E.K. Hulet, J.F. Wild, R.J. Dougan, R.W. Lougheed, J.H. Landrum, A.D. Dougan, P.A. Baisden, C.M. Henderson, R.J. Dupzyk, R.L. Hahn, M. Schädel, K. Sümmerer, and G.R. Bethune, Phys. Rev. **C40**, 770 (1989).

[15] G.T. Seaborg and W.D. Loveland, *The elements beyond uranium* (J. Wiley, New York 1990).

[16] S. Hofmann, in *Proc. Int. Conf. "Actinides-93"*, Santa Fe (USA), 1993, J. Alloys and Compounds, in press.

[17] R.W. Lougheed, K.J. Moody, J.F. Wild, E.K. Hulet, J.H. McQuaid, Yu.A. Lazarev, Yu.V. Lobanov, Yu.Ts. Oganessian, V.K Utyonkov, F.Sh. Abdullin, G.V. Buklanov, B.N. Gikal, S. Iliev, A.N. Mezentsev, A.N. Polyakov, I.M. Sedykh, I.V. Shirokovsky, V.G. Subbotin, A.M. Sukhov, Yu.S. Tsyganov, and V.E.Zhuchko, in *Proc. Int. Conf. "Actinides-93"*, Santa Fe (USA), 1993, J. Alloys and Compounds, in press.

[18] Yu.A. Lazarev, Yu.V. Lobanov, Yu.Ts. Oganessian, V.K Utyonkov, F.Sh. Abdullin, G.V. Buklanov, B.N. Gikal, S. Iliev, A.N. Mezentsev, A.N. Polyakov, I.M. Sedykh, I.V. Shirokovsky, V.G. Subbotin, A.M. Sukhov, Yu.S. Tsyganov, V.E.Zhuchko, R.W. Lougheed, K.J. Moody, J.F. Wild, E.K. Hulet, and J.H. McQuaid, Phys. Rev. Lett. **73**, 624 (1994).

[19] P. Armbruster, in *Proc. Int. Conf.: "Nuclear Shapes and Nuclear Structure at Low Excitation Energies"*, Antibes (France), 1994, in press.

[20] R. Smolańczuk, J. Skalski, and A. Sobiczewski, in *Proc. Int. School-Seminar on Heavy Ion Physics*, Dubna (Russia), 1993, eds. Yu.Ts. Oganessian, Yu.E. Penionzhkevich, and R. Kalpakchieva, vol. 1 (JINR, Dubna, 1993), p. 157.

[21] R. Smolańczuk, J. Skalski, and A. Sobiczewski, in *Proc. NATO Advanced Course: "Frontier Topics in Nuclear Physics"*, Predeal (Roumania), 1993, eds. W. Scheid and A. Sandulescu (Plenum), in press.

[22] A. Sobiczewski, R. Smolańczuk, and J. Skalski, in *Proc. Int. Conf. "Actinides-93"*, Santa Fe (USA), 1993, J. Alloys and Compounds, in press.

[23] H.J. Krappe, J.R. Nix, and A.J. Sierk, Phys. Rev. **C20**, 992 (1979).

[24] P. Möller and J.R. Nix, Nucl. Phys. **A361**, 117 (1981); At. Data Nucl. Data Tables **26**, 165 (1981).

[25] S. Ćwiok, J. Dudek, W. Nazarewicz, J. Skalski, and T. Werner, Comput. Phys. Commun. **46**, 379 (1987).

[26] A. Sobiczewski, Z. Szymański, S. Wycech, S.G. Nilsson, J.R. Nix, C.F. Tsang, P. Möller, and B. Nilsson, Nucl. Phys. **A131**, 67 (1969).

[27] M. Brack, J. Damgaard, A.S. Jensen, H.C. Pauli, V.M. Strutinsky, and C.Y. Wong, Rev. Mod. Phys. **44**, 320 (1972).

[28] K. Pomorski, T. Kaniowska, A. Sobiczewski, and S.G. Rohoziński, Nucl. Phys. **A283**, 394 (1977).

[29] A. Sobiczewski, Sov. J. Part. and Nuclei **10**, 1170 (1979).

[30] H.C. Pauli, Phys. Reports **C7**, 35 (1973); Nukleonika **20**, 601 (1975).

[31] S.E. Larsson, Phys. Scr. **8**, 17 (1973).

[32] R. Smolańczuk, H.V. Klapdor-Kleingrothaus, and A. Sobiczewski, Acta Phys. Pol. **B24**, 685 (1993).

[33] A. Sobiczewski, Z. Patyk, S. Ćwiok, and P. Rozmej, Nucl. Phys. **A485**, 16 (1988).

[34] M. Schädel, private communication.

[35] G.M. Ter-Akopyan, A.S. Iljinov, Yu.Ts. Oganessian, O.A. Orlova, G.S. Popeko, S.P. Tretyakova, V.I. Chepigin, B.V. Shilov, and G.N. Flerov, Nucl. Phys. **A255**, 509 (1975).

[36] F.P. Hessberger, G. Münzenberg, S. Hofmann, W. Reisdorf, K.H. Schmidt, H.J. Schött, P. Armbruster, R. Hingmann, B. Thuma, and D. Vermeulen, Z. Phys. **A321**, 317 (1985).

[37] L.P. Somerville, M.J. Nurmia, J.M. Nitschke, A. Ghiorso, E.K. Hulet, and R.W. Lougheed, Phys. Rev. **C31**, 1801 (1985).

[38] G. Münzenberg, S. Hofmann, H. Folger, F.P. Hessberger, J. Keller, K. Poppensieker, B. Quint, W. Reisdorf, K.H. Schmidt, H.J. Schött, P. Armbruster, M.E. Leino, and R. Hingmann, Z. Phys. **A322**, 227 (1985).

[39] S. Hofmann et al., to be published.

[40] S. Hofmann, private communication.

[41] P. Möller and J.R. Nix, Preprint LA-UR-93-2221; J. Phys. G, in press.

[42] A. Sobiczewski, Z. Patyk and S. Ćwiok, Phys. Lett. **B224**, 1 (1989).

[43] P. Armbruster, Ann. Rev. Nucl. Part. Sci. **35**, 135 (1985).

[44] P. Armbruster, in *Proc. Int. School on Heavy Ion Physics*, Erice (Italy), 1986, eds. R.A. Broglia and G.F. Bertsch (Plenum Press, New York, 1988), p. 153.

[45] W.D. Myers and W.J. Swiatecki, Nucl. Phys. **81**, 1 (1966).